1981

Mott g-Ratios in Rbx(NH3)1-x and Oxidation state of Rubidium Compounds from XAS

Juana Vivó Acrivos, *San Jose State University*
K. Hathaway, *San Jose State University*
A. Robertson, *University of California - Berkeley*
M. P Klein, *University of California - Berkeley*
A. Thompson, *University of California - Berkeley*

J. Phys. C: Solid State Phys., **14** (1981) L557–L564. Printed in Great Britain

LETTER TO THE EDITOR

Mott *g*-ratios in $Rb_x(NH_3)_{1-x}$ and oxidation state of rubidium compounds from XAS

J V Acrivos†, K Hathaway†, A Robertson‡, A Thompson‡ and M P Klein‡

† San José State University, San José, California 95192, USA

‡ University College, Berkeley, California 94305, USA

Received 23 April 1981

Abstract. The x-ray absorption spectra (XAS) of Rb metal, $Rb_x(NH_3)_{1-x}$, 2H-$NbSe_2Rb_{0.28}$ and RbBr near the Rb K-edge have been used to ascertain that the oxidation state V of rubidium dissolved in ammonia and intercalated in the layer compound is in the range $0 < V < 1$. The observed edge shifts with temperature for semimetals are explained in terms of the population of band states, and the ratio of the density states near the mobility edge over that calculated for a free electron model, i.e. the Mott ratio g, is ascertained using a semiempirical relation developed for the x-ray absorbance from 1s levels to empty states near the mobility edge.

XAS is traditionally divided into an XAES region where the ejected electron transitions to bound states are observed (the so-called absorption edge) and an EXAFS region (10^2 to 10^3 eV above the latter, the so-called extended x-ray absorption fine structure region) where transitions to free electron states are observed (Kronig 1932, Hartree *et al* 1934, Stern *et al* 1975). The XAES region contains information on the oxidation state of the absorber and recent semiempirical relations have shown that the edge position increases linearly with say the valence of Mn, Fe, Mo, Rb and Sr (Cramer *et al* 1976, J A Kirby unpublished, Acrivos *et al* 1980). Also transitions to bound states of the absorber can be resolved, e.g.

$$(Z^v)\ (1s)^2 \ldots : {}^{2S+1}L_J \rightarrow (Z^v)\ (1s) \ldots nl : {}^{2S+1}(L \pm 1)_{J+1} \qquad (1)$$

where ... represents other core electrons not directly involved in the transition and the nl states are members of a Rydberg series for a given angular momentum l including the exciton states. Parratt and others (Parratt 1939, 1959, Cauchois and Mott 1949) have related the spacings between the series of transitions (1) with those reported in the literature for the element with atomic number $Z + 1$ and a closed K shell, i.e.

$$((Z+1)^v)\ (1s)^2 \ldots n'l' : {}^{2S'+1}L'_{J'} \rightarrow ((Z+1)^v)\ (1s)^2 \ldots nl : {}^{2S'+1}L''_{J''} \qquad (2)$$

where $S' = S \pm \frac{1}{2}$ and this valuable approximation is correct if exchange interactions between the K electrons and the other core electrons are negligible. In this work we make use of the XAES data including the edge position and the transitions (1) in order to ascertain the valence of rubidium in the metal–ammonia solutions (MAS) and in intercalated compounds for the purpose of determining the metallic nature of the system.

0022-3719/81/190557 + 08 $01.50

The XAES data for Rb metal, RbBr, $RbN_3$and Rb MAS and for $2H\text{-}NbSe_2Rb_{0.28}$ were reported previously (Acrivos *et al* 1980, Bourdillon *et al* 1979). Here figure 1 shows that the edge inflection point E_i moves to higher energy by 4.5 eV as the valence increases from 0 in Rb metal to +1 in RbBr and RbN_3, displaying an intermediate value for Rb MAS. The edge positions for the intercalated compounds were not determined with the same standards (Bourdillon *et al* 1979); however, the most useful observations are

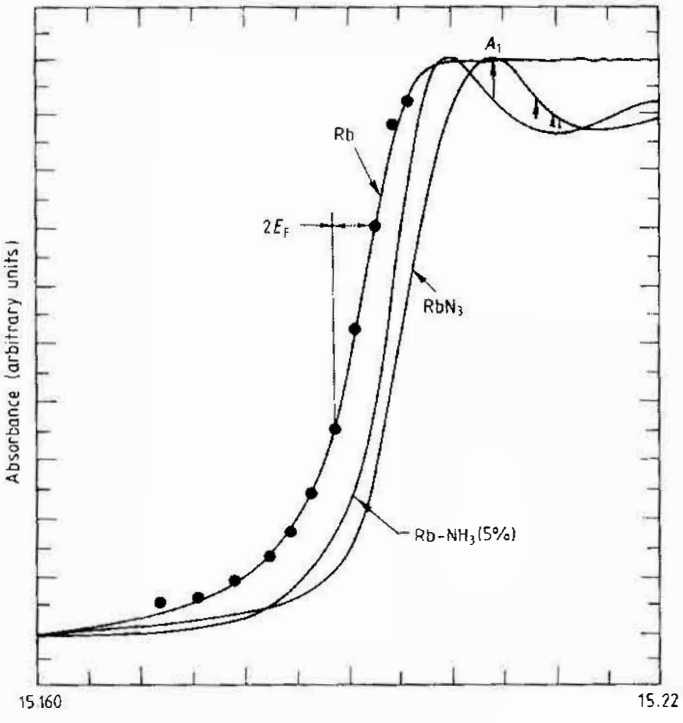

Figure 1. XAES for different Rb compounds. A_m^0 evaluated using equation (4) with E_F = 1.79 eV is indicated by dots.

related to transitions (1), i.e.

$$(Rb^{+1})\ (1s)^2\ .\ .\ .\ :\ {}^1S_0 \rightarrow (Rb^{+1})\ (1s)\ .\qquad np:\ {}^1P_1 \tag{1'}$$

where $n \geqslant 5$. The spacing in the Rydberg series $n = 5, 6, 7, 8$ can be estimated from transitions (2) in the literature (Moore 1952) for Sr^{+1}, i.e.

$$(Sr^{+1})\ (1s)^2\ .\ .\ .\ 5s:\ {}^2S_{1/2} \rightarrow (Sr^{+1})\ (1s)^2\ .\ .\ .\ np:{}^2P_{1/2,3/2} \tag{2'}$$

which are indicated by arrows in figure 1 for RbN_3.

Now the changes in absorbance against T for MAS have to be explained. A semiempirical analysis shows how the variation in the density of states may be extracted from the temperature dependence of the absorbance as follows. In non-metals (NM) the transitions to a continuum of free states from a 1s level give rise to an infinite sum of

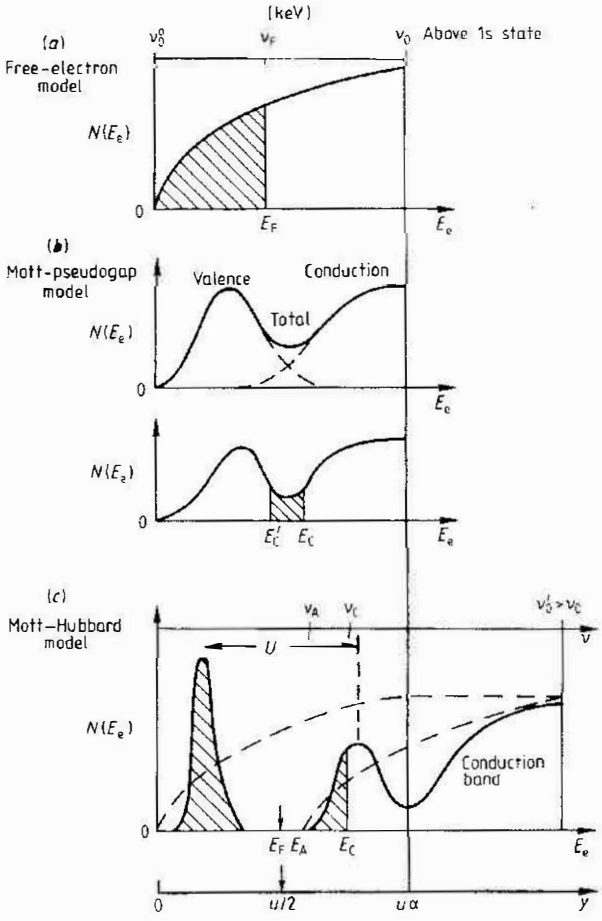

Figure 2. Density of states for different models according to Mott (1974).

Lorentzian curves which start at the edge $E_0 = h\nu_0$ in figure 2, i.e. the absorbance is (Richtmyer *et al* 1934)

$$A_{nm}(\nu) = D_\nu(\pi/2 + \theta_{nm}) \tag{3}$$

shown in figure 3. Here $-\pi/2 \leqslant \theta_{nm} = \tan^{-1}[2\pi T_\nu(\nu - \nu_0)] \leqslant \pi/2$ and $D_{\nu'\nu} = D_\nu$ is a function of the transition probability and the joint density of states and T_ν is a lifetime depending on the initial and final state widths. Then the XAES for Rb^+ in figure 1 are explained as a series of Rydberg transitions (1) (each described by a single Lorentzian which decreases in intensity by a factor greater than two from the previous one in the series) plus (3).

In alkali metals (or alkaline earth metals) the conduction electrons occupy band states and these affect both transitions (1) and (2) as follows. The band states are occupied up to the Fermi level $E_F = k_F^2/2m = h(\nu_F - \nu_0^0)$ where ν_0^0 is the bottom of the conduction band and ν_F is the Fermi level in figure 2(*a*). However, ν_F may be in the vicinity of the final states in transition (1). In this case mixing of localised and extended

states can and does occur (Fano 1961), leading to occupancy of the final states in transition (1) and to the absence of exciton states. The overall absorbance is then written:

$$A(\nu) = A_1(\nu) + A_{nm}(\nu) \tag{4}$$

where A_{nm} is given by equation (3), and in order to ascertain which of the different models shown in figure 2 describes the MAS correctly we write the absorbance below the

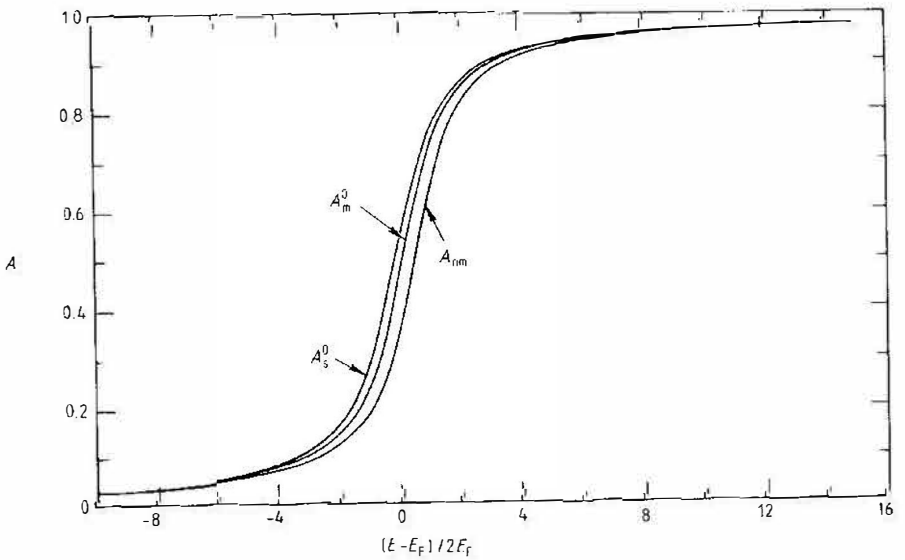

Figure 3. Normalised absorbance A^0 against $(E - E_F)/2e_F$ with $\alpha, u \approx 1$ in equation (4).

edge separately:

$$A_1 = D_\nu \int_{\nu_0^0}^{\nu_0} \frac{2\pi T_\nu d\nu'(1-f)}{1 + 4\pi^2(\nu' - \nu)\,T_\nu^2} N(\nu')/N(\nu_0).$$

f is the Fermi distribution function for the occupation of a level in figure 2, and the density of states $N(\nu')$ has been normalised to the value at ν_0 for the metal and $D_{\nu'\nu}$ has been replaced by D_ν. For a spherical Fermi surface the density of states near the bottom of the conduction band varies as the square root of the kinetic energy, i.e.

$$N(\nu')/N(\nu_0) = [(\nu' - \nu_0^0)/(\nu_0 - \nu_0^0)]^{1/2}$$

and as exciton states appear variations in A_1 are expected as one goes from a metal to an insulator.

The physical significance of A_1 may be ascertained by introducing dimensionless variables y in units of $2E_F$ in equation (4) ($y = y(\nu) \equiv uh(\nu - \nu_0^0)/2E_F$) as shown in figure 2, where the uncertainty principle requires that $T_\nu E_F \geq \hbar/2$ and defines the parameter $u \equiv 2T_\nu E_F/\hbar \geq 1$. Then

where $y' = x - i + y$ and the edge will vary as a function of f as follows:

(*a*) For semiconductors near 0 K, $f = 0$ in equation (4), and the integral is evaluated using relation 2.225 of Gradshteyn and Ryzhik (1965) to give the semiconductor edge absorbance, A_s^0, plotted in figure 3. However, as T increases $(1 - f) \leq 1$ in equation (4) causes the edge to move to higher energy as shown in figure 4 for Rb-NH_3, which is discussed below.

(*b*) For metals when $E_F \gg k_B T$, $f = 1$ in (4) for $0 < y' < u/2$ and $f = 0$ when $y > u/2$, giving rise to the metallic edge absorbance, A_m^0, plotted in figure 3. The calculated points A_m^0 have been plotted over the experimental Rb metal edge in figure 1 using $E_F(\mathrm{Rb}) = 1.79$ eV to show the type of agreement obtained.

(*c*) For semimetals the absorbance is somewhere between A_s^0 and A_m^0 above. At finite temperatures, if E_g is an activation energy from a valence to a conduction band, the absorbance is written by adding a term to A_m^0, i.e.

$$A_s = A_m^0 + \int_0^{u/2} (1 - f)\, dA^0 \exp(-\beta E_g) \tag{5}$$

which can be integrated by parts to obtain the semiconductor edge absorbance A_s, at finite temperature $(\beta = 1/k_B T)$:

$$A_s = A_s^0 - \left[A_s^0 - A_m^0 + 2\beta E_F \int_0^{u/2} A^0 f(1 - f)\, dy'\right] \exp(-\beta E_g). \tag{6}$$

For a semiconductor $f(1 - f)$ is negligible and in a first approximation the last term in equation (6) is dropped, i.e.

$$A_s^{(1)}(y, T) \equiv A_s^0[1 - r \exp(-\beta E_g)] \tag{7}$$

where $r = (A_s^0 - A_m^0)/A_s^0$ is the fractional reduction of the absorbance due to the population of states between the bottom of the conduction band and ν_0' and the magnitude of r evaluated from equation (4) is ~0.2 near ν_F. The edge absorbance changes with β as

$$(\partial \ln A_s^{(1)}/\partial\beta)_y = E_g(A_s^0 - A_s^{(1)})/A_s^{(1)} \tag{8}$$

and the magnitude of y near the edge inflection point increases with T, because in equation (7)

$$A_s^{(1)}(y, T)/A_s^0(y, 0\,\mathrm{K}) = 1 - r \exp(-\beta E_g) < 1 \tag{7'}$$

causing the shifts observed in figure 4. When $T = -56°$ to $-10°$C for Rb-NH_3 (5 MPM) in figure 4 the slope $(\partial \ln A/\partial\beta)_y = 4 \times 10^{-3}$ eV to 2×10^{-2} eV gives an energy $E_g \geq 0.26$ eV. This is unrealistically high, indicating that the simple band model in figure 2(*a*) does not apply to MAS near the metal–insulator transition. Other band models must be considered.

(*d*) Mott has described various cases for the calculation of the density of states in disordered materials as shown in figure 2. The conductivity in MAS has been described qualitatively by $N(E_c)$ forming two overlapping bands where localised states are occupied up to say $E_{c'}$ in figure 2(*b*) (Mott 1974). Then the absorbance must be written with a correction for the density of states, i.e.

$$A_g(y) = A_{1g}(y) + A_{nn}(y) \tag{9}$$

where

$$A_{1g}(y) = \int_{y_{c'}}^{ua} g(\nu')\, dA^0$$

where $y_{c'} = E_{c'}/2E_F$ and $g(\nu') = N(\nu')/N(\nu')_{\text{free electrons}}$ is the ratio of the density of states relative to that for a free electron gas, i.e. $g_c < 1$ near $\nu = \nu_c$ is the Mott ratio and $g \to 1$ as $\nu \to \nu_0$. Integration by parts then gives

$$A_g(y) = A_s^0 - g_c(A_s^0 - A_m^{\bullet}) - \int_{y_{c'}}^{u\alpha} A^{(}\,\mathrm{d}g \tag{9'}$$

and the absorbance correct to first order, neglecting the last term in equation (9'), is

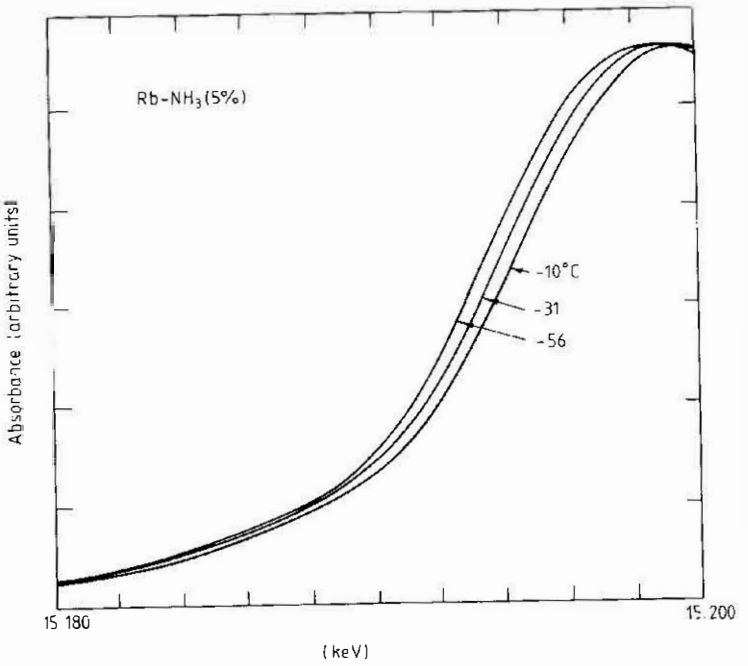

Figure 4. XAFS of Rb-NH_3, 5 MPM at different T. Here $A = 83.1; 78.2$ and 67 are the averages of different measurements near 15.193 keV at −56, −31 and −10°C respectively.

written in a form similar to equation (7), i.e.

$$A_g^{(1)}(y) = A_s^0(y)\,(1 - g_c r) \tag{10}$$

where E_g in equation (7) has been replaced in equation (10) by $-(\partial \ln g_c/\partial\beta)$, which is not constant with β (i.e. $g \to 0$ as $\beta \to \infty$). We apply equation (10) to the data in figure 4 (5 MPM Rb-NH_3 with $r = 0.2$). Then, $g_c(-31°C) - g_c(-56°C) = 0.3$ and $g_c(-10°C) - g_c(-56°C) = 0.9$ support a density of states shape given by figure 2(b). Here $g_c(-56°C) \leqslant 0.2$ was evaluated from conductivity data (Sharp *et al* 1971).

Other models which predict a density of states which changes with temperature near the mobility edge, such as the Mott–Hubbard model in figure 2(c), would also explain the absorbance near ν_F or ν_c. Here, if the density of states decreases for E_c above E_c as in figure 2(c), the absorbance should show additional structure above the onset of the continuum of states. Also, when $\nu_0' \gg \nu_0$ in figure 2(c) and the edge is identified near ν_c, the decrease in the density of states as $E_c > E_c$ would affect the EXAFS relation. Here

the amplitudes measured relative to $A(\nu_c)$ would give a smaller number of scatterers about the absorber. This has been observed in M-NH_3 (Acrivos *et al* 1980) but a qualitative interpretation of results may be accomplished with the $N(E_c)$ given in either figure 2(*b*) or 2(*c*).

In summary, relations (4) are to be compared with the data in figures 1 and 4 as follows:

(i) The value $E_F(Rb) = 1.79$ eV used in relation (4) fits the XAES date for Rb metal in figure 1 in the region where D_ν is not expected to change very fast. Here it is interesting to note that the edge sharpness depends on E_F alone if the uncertainty principle gives $T_\nu E_F \geqslant \hbar/2$, which assumes that the width of the final states is greater than that for the 1s initial state.

(ii) E_F for $Rb_{0.05}(NH_3)_{0.95}$ has been estimated to be 0.4 eV (Thompson 1976, 1977, Sharp *et al* 1971), but the $T = 0$ absorbance A_s^0 evaluated using equation (4) is much sharper than the observed edge in figure 1. This is probably due to temperature effects.

(iii) The Rb edge in 2H-$NbSe_2Rb_{0.28}$ (Bourdillon *et al* 1979) shows exciton structure similar to A of MAS not Rb metal in figure 1 suggesting that the intercalated layer is not metallic. The reason for this may arise from two possibilities: (*a*) the Rb atoms have been separated in the intercalated layer causing a true Mott transition (Mott 1974); or (*b*) charge transfer may have occurred from the Rb layer into the $NbSe_2$ layer. The accurate edge position and its T dependence is necessary to determine which of these two possibilities is correct.

In conclusion, it has been shown that XAES data can be used to ascertain the nature of metal–insulator transitions in semimetals such as M-NH_3 and intercalated layer materials where it is not possible to use other conventional methods. This is of some importance in order to ascertain the metallic properties of intercalated compounds and M-NH_3 where the metallic properties of the constituent layers are different and where other measurements, e.g. Knight shift data, give only an average g-ratio over all the collisions occurring in 10^{-10} s (Acrivos and Mott 1971). Also, the Mott ratio which is proportional to the conductivity squared can be evaluated from experimental data only for values above minimum metallic conductivity of 200 $(\Omega\ \mathrm{cm})^{-1}$ but g_c can be evaluated from equation (10) for any metal concentrations and serves to show for the first time how thermal disorder leads to increase the overlap between two Hubbard bands.

This work was carried out under the auspices of NSF Grant DMR 7820577 and by the Biomedical and Environmental Research Division of DOE under contract W-7405-Eng-48 and SSRL Proposals 76 and 312. The facilities at SSRL are supported under NSF contract DMR 77-27489 in cooperation with the US Department of Energy. We also acknowledge the help and enthusiasm of fellow workers J Kirby, L Esparza, J Code, J Reynolds and S Brown. J V Acrivos is grateful for the interest shown in this work by N F Mott and J C Thompson.

References

Acrivos J V, Hathaway K, Robertson A C, Thompson A and Klein M P 1980 *J. Phys. Chem.* **84** 1206
Acrivos J V and Mott N F 1971 *Phil. Mag.* **24** 19
Bourdillon A J, Pettifer R F and Marseglia E A 1979 *J. Phys. C: Solid State Phys.* **12** 3889
Cauchois Y and Mott N F 1949 *Phil. Mag.* **40** 1250
Cramer S P, Eccles T K, Kutzler F, Hodgson K O and Doniach S 1976 *J. Am. Chem. Soc.* **98** 8059

Fano U 1961 *Phys. Rev.* **124** 1866
Gradshteyn I S and Ryzhik I M 1965 *Tables of Integrals* (New York: Academic Press)
Hahne S and Schindewolf U 1975 *J. Phys. Chem.* **79** 2922
Hartree D R, Kronig R de L and Petersen H 1934 *Physica* **1** 895
Kirby J A unpublished
Kronig R de L 1932 *Z. Phys.* **75** 191, 468
Moore C E 1952 *'Atomic Energy Levels': NBS Circular* 467
Mott N F 1974 *Metal–Insulator Transitions* (Cambridge: CUP)
Parratt L G 1939 *Phys. Rev.* **56** 295
—— 1959 *Rev. Mod. Phys.* **31** 616
Richtmyer F K, Barnes S W and Ramberg E 1934 *Phys. Rev.* **46** 843
Sharp A C, Davis R L, Van der Hoff J A, Le Master E W and Thompson J C 1971 *Phys. Rev.* **4**A 414
Shulman R G, Yafet Y, Eisenberger P and Blumberg W E 1976 *Proc. Nat. Acad. Sci., USA* **73** 1384
Stern E A, Sayers D E and Lytle F W 1975 *Phys. Rev.* **15**B 4836
Thompson J C 1976 *Electrons in Liquid Ammonia* (Oxford: Clarendon)
—— 1977 *Solutions Metal Ammoniac* ed G Lepoutre and M J Sienko p 307

Appendix: glossary of terms used

MAS metal–ammonia solutions
XAS x-ray absorption spectroscopy
XAES x-ray edge absorption spectroscopy
V valence of absorber
Z atomic number of absorber
A absorbance of x-rays by a given material:
- A_{nm} for non-metals
- A_s for semimetals
- A_m for metals
- A_g for materials with overlapping bands
- A^0 for material near 0 K
- $A^{(1)}$ first-order approximation (neglecting $(1-f)f \ll 1$ and/or $dg \approx 0$)
- $A_1 = A - A_{nm}$ absorbance below the edge E_0.

ν Frequency of x-ray photons measured from the 1s level of absorber:
- ν_0^0 to the bottom of the conduction band
- ν_F to the Fermi level
- ν_0 to the edge of the continuum of free states in non-metals ($E_0 = h\nu_0$)
- $y = y(\nu) = h(\nu - \nu_0^0)/2E_F\, u^{-1}$: dimensionless parameter which measures the photon energy from the bottom of the conduction band in units of a resonance line half-width at half height ($\hbar/T_\nu = 2E_t/u$).

$N(\nu)$ density of states near $E = h\nu$ above the 1s level of the absorber
D_ν relative intensity of resonance line near $E = h\nu$
$2E_g$ activation energy in simple semimetal
g_c Mott ratio g measured near the mobility edge.